

## NEURODEGENERATIVE DISEASES

# Response to Comment on “Microglial activation states drive glucose uptake and FDG-PET alterations in neurodegenerative diseases”

Xianyuan Xiang<sup>1,2</sup>, Sabina Tahirovic<sup>3</sup>, Sibylle Ziegler<sup>4,5</sup>,  
Christian Haass<sup>1,3,5\*</sup>, Matthias Brendel<sup>3,4,5\*</sup>

Microglial FDG uptake alterations are the source of FDG-PET changes in models of neurodegenerative diseases.

Copyright © 2022  
The Authors, some  
rights reserved;  
exclusive licensee  
American Association  
for the Advancement  
of Science. No claim  
to original U.S.  
Government Works

With great interest, we have recognized the technical comment of Zimmer *et al.* on our recent *Science Translational Medicine* paper by Xiang *et al.* (1). We appreciate the discussion on the cellular origin of the fluorodeoxyglucose positron emission tomography (FDG-PET) signal, and given the many remaining open questions, we hope that this will stimulate further important research in this area. We fully agree with Zimmer *et al.* that astrocytes play an important role in FDG uptake of the brain, and we did not deny the contribution of astrocytic FDG uptake as one major source of the overall FDG-PET signal. However, considering the recent data from another group (2), together with our findings (1), a substantial direct contribution of microglial FDG uptake to the FDG-PET signal specifically after triggering receptor expressed on myeloid cells 2 (TREM2)-dependent activation is important to consider.

First, in the technical comment, Zimmer *et al.* suggest that the total microglia cell number could be too low to influence the total FDG-PET signal. However, our data clearly indicate that microglia are responsible for the FDG-PET increases in amyloid mouse models and decreases in *Trem2*-knockout (TREM2-KO) mice and that microglia account for ~10% of the total FDG uptake in the healthy mouse brain. Microglial contribution to FDG uptake was determined by the magnitude of PET signal decrease after 99% microglia depletion in wild-type mice. We reevaluated our data after cross-calibration of absolute activity in isolated cells and the activity of the whole brain before isolation. We now provide an additional FDG allocation model that accounts for single microglia cell uptake as assessed by magnetic-activated cell sorting after tracer injection (1), considering the mentioned 7% microglia cells in mouse brain (Fig. 1, A and B) (3). Here, we find an excellent confirmation of the relative contribution of microglia to the total FDG-PET uptake between PET (9.8% reduction at 99% depletion) and magnetic-activated cell sorting (MACS; 8.6%; Fig. 1C). The excellent agreement between estimates of the microglial contribution to the total FDG uptake between PET (29.1%) and MACS (29.9%) was also observed for the  $\beta$ -amyloid mouse model, assuming a 1.3-fold increase in microglial density (1) due to proliferation

(Fig. 1B). Together with the fact that the uptake in an amyloid model is TREM2 dependent, this cross-validation makes it very likely that the elevation of FDG-PET in our study derived from the elevated FDG uptake of microglia cells and not from other cell types. In line, microglia depletion in wild-type animals does not overtly change astrocytic phenotypes (4), such that the reduced FDG-PET signal can likely be attributed to microglia. Our findings of elevated microglial FDG uptake in the amyloid mouse model when compared to wild type were independently validated in the 5xFAD mouse model of Alzheimer's disease (AD) in a separate manuscript (2). Moreover, in this study, using MACS and single-cell RNA sequencing, higher glucose uptake and altered glucose metabolism signatures were observed in hippocampal microglia but not in hippocampal nonmicroglia cells (2). Thus, we conclude that microglia, and not astrocytes, are predominantly responsible for the FDG alterations in amyloid mouse models because amyloid-driven changes in FDG uptake are dependent on TREM2, which, within the brain, is exclusively expressed in microglia.

Second, Zimmer *et al.* mention that microglial activation could influence astrocytic glucose uptake as an alternative model to an elevated direct glucose uptake by microglia. Estimated astrocytic FDG uptake by MACS in the FDG allocation model was lower (2.2% of the total brain) when compared to microglia, but we believe that a relevant proportion of FDG in astrocyte processes is likely missed due to loss of processes during the dissociation procedure (Fig. 1, A and B). Recent data of FDG-PET signal reduction after clozapine-induced glutamate transporter 1 blockade (5) indicate that astrocytic FDG uptake could comprise a magnitude of  $\geq 20\%$  of the whole brain. Therefore, we fully agree that contributions of astrocytes, especially astrocytic processes, need to be acknowledged when interpreting brain FDG-PET imaging (6). However, the additional findings presented here show that microglia incorporated glucose to a higher degree in  $\beta$ -amyloid mouse models in a TREM2-dependent manner (1, 2). This again suggests a direct contribution of microglia to the FDG-PET signal that does not derive from microglia-dependent activation of astrocytes via cytokines, because TREM2 loss of function would then be expected to modulate astrocytic FDG uptake, which is not the case (7). Nevertheless, we fully agree that astrocytes potentially have a strong overall contribution to the basal FDG-PET signal.

Third, Zimmer *et al.* claim that the astrocyte isolation method used did not capture the entire astrocyte population. We agree that capturing all astrocytes is a big challenge in the field. The anti-CD11b antibody was used to isolate the whole population of microglia/macrophages, and the anti-astrocyte cell surface antigen-2 (ACSA-2) antibody was used to isolate astrocytes. However, ACSA-2 is coexpressed on all astrocytes with bona fide markers such as

<sup>1</sup>Biomedical Center (BMC), Division of Metabolic Biochemistry, Faculty of Medicine, Ludwig-Maximilians-Universität München, 81377 Munich, Germany. <sup>2</sup>CAS Key Laboratory of Brain Connectome and Manipulation, the Brain Cognition and Brain Disease Institute, Shenzhen Institutes of Advanced Technology, Chinese Academy of Sciences, Shenzhen-Hong Kong Institute of Brain Science-Shenzhen Fundamental Research Institutions, Shenzhen 518055, China. <sup>3</sup>German Center for Neurodegenerative Diseases (DZNE) Munich, 81377 Munich, Germany. <sup>4</sup>Department of Nuclear Medicine, University Hospital of Munich, LMU Munich, 81377 Munich, Germany. <sup>5</sup>Munich Cluster for Systems Neurology (SyNergy), 81377 Munich, Germany.  
\*Corresponding author. Email: christian.haass@mail03.med.uni-muenchen.de (C.H.); matthias.brendel@med.uni-muenchen.de (M.B.)

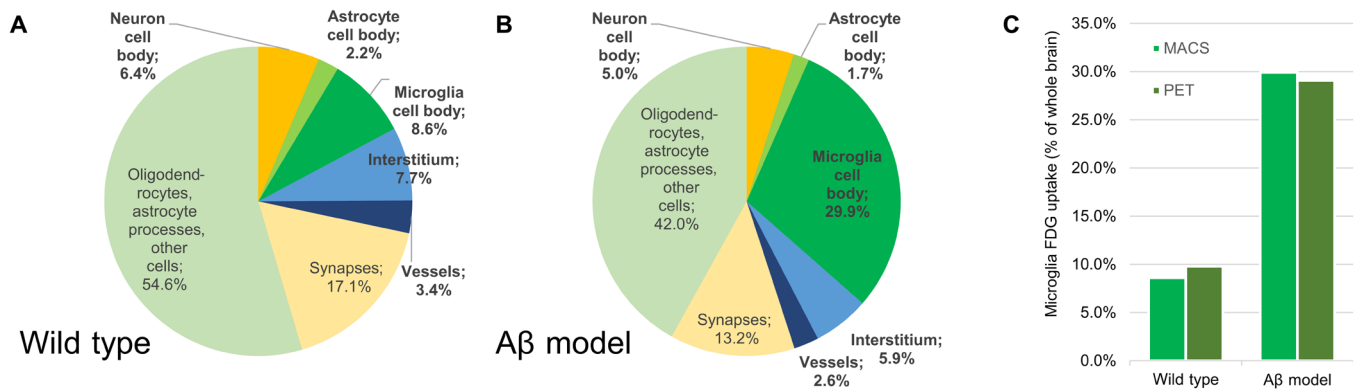


**Fig. 1. Hypothetical model of [ $^{18}\text{F}$ ]FDG distribution in the mouse brain at 30 min p.i. in wild-type mice in comparison to an  $\text{A}\beta$  model. (A and B)** Single-cell [ $^{18}\text{F}$ ]FDG uptake (% per brain dose; after cross-calibration of cell pellet and total brain measures) as assessed by magnetic-activated cell sorting (MACS) (1) was multiplied with published total cell numbers in the mouse brain, comprising  $7.1 \times 10^6$  neurons (11) or 7% ( $\approx 7.6 \times 10^6$ ) microglia cells (3). Interstitial [ $^{18}\text{F}$ ]FDG was estimated by interstitial compartment volume (12) and assumed equilibrium of nonphosphorylated extra- and intracellular [ $^{14}\text{C}$ ]deoxyglucose (13) and the known ratio of [ $^{14}\text{C}$ ]deoxyglucose and [ $^{14}\text{C}$ ]deoxyglucose-6-phosphate at 30 min p.i. (14). Vessel [ $^{18}\text{F}$ ]FDG was estimated by cerebral vessel volume (15) and known activity concentration of plasma relative to tissue at 30 min p.i. (16). Synaptic [ $^{18}\text{F}$ ]FDG uptake was estimated via an enriched synaptosome fraction relative to the [ $^{18}\text{F}$ ]FDG uptake of whole-brain homogenate. The remaining [ $^{18}\text{F}$ ]FDG uptake was assumed to be located in oligodendrocytes (17), cell processes (predominantly astrocytic), and other cell types. A microglia proliferation index of 1.3 was assumed for the whole brain in the  $\beta$ -amyloid ( $\text{A}\beta$ ) mouse model (1). (C) Estimated cellular microglial [ $^{18}\text{F}$ ]FDG uptake as assessed by MACS was cross-validated with observed %TSPO-PET reductions after microglia depletion (1).

aldehyde dehydrogenase 1 family member L1 (Aldh1l1), glial fibrillary acidic protein (GFAP), S100 calcium-binding protein B, and glutamate-aspartate transporter. Aldh1l1-Cre/ERT2 animals are widely used as a model to drive gene expression in the vast majority of astrocytes. However, we cannot exclude that by using the anti-ACSA-2 antibody isolation strategy, we are losing a subset of ACSA-2-negative astrocytes, which could, in turn, display altered glucose uptake. Still, the aforementioned direct effects of altered FDG uptake in single microglial of  $\beta$ -amyloid and TREM2-KO mouse speak for microglia-driven FDG uptake alterations in the investigated disease situations.

Fourth, Zimmer *et al.* mention that the translocator protein 18 kDa (TSPO)-PET signal could also derive from astrocytes instead of microglia as its specific source. We agree that TSPO is not a microglia-specific marker because both microglia and astrocyte displayed increases in TSPO in an amyloid rat model and in AD subjects (8). However, PET and autoradiography studies using new-generation TSPO tracers such as [ $^{18}\text{F}$ ]GE-180 and [ $^{11}\text{C}$ ]PBR28 in mouse models of amyloidosis have shown high specificity and correlations of these tracers with microglia (9, 10). Furthermore, immunohistochemistry analysis with antibodies against TSPO has shown no or rare staining in astrocytes (using different markers for astrocytes besides GFAP), both in AD mouse models and in AD human brains, although demonstrating some signal in endothelial cells lining the blood vessels and the epithelial cells forming the choroid plexus (9, 10). In addition, we observed an excellent correlation between TSPO-PET and immunohistochemical markers for activated microglia in mice. Therefore, both microglia and astrocyte contribute to the TSPO-PET signal. However, we observed a TREM2-dependent increase in glucose uptake in amyloid mouse models, which suggests a selective increase in FDG in microglia. Although the situation is certainly more complicated in human brains, our combined data suggest that microglial FDG uptake will also play a considerable role in patients.

As a general remark, our proposed FDG allocation model of all brain compartments is complex (Fig. 1), and we refrained to overextrapolate

our existing data for that reason (1). However, determining a model of all cellular sources of the entire FDG uptake in the brain is, in principle, feasible and deserves further investigation. Brain dissociation and sorting of different cell types and cell fragments after radiotracer injection (“radiosorting”) allow the specific localization of trapped FDG throughout the brain, resulting in FDG uptake per unit such as cell number or mass of protein. Sources that could be lost during the dissociation and sorting process, particularly synapses and oligodendrocytes, need to be taken into account for this calculation. In addition, sorted material only contains a snapshot of the full cell population or mass availability in the brain, and additional data or literature are needed to define their quantitative abundance (3). Nonetheless, our data of single-cell FDG uptake in microglia already indicated feasibility to recapitulate the changes of FDG-PET induced by amyloidosis or TREM2 deficiency at a cell population level. We fully agree that the human situation is more complex and more difficult to disentangle because FDG uptake measures at the single-cell level are challenging.

In summary, there is growing evidence that not only neurons but also astrocytes and microglia contribute relevantly to glucose uptake and the resulting radioactive PET snapshot of FDG accumulation in the brain. Neurodegenerative diseases strongly affect glial FDG uptake and glial metabolism. The combined data should increase the awareness to consider glia cells as key contributors of FDG uptake, and the detailed proportions of these cellular contributions in healthy brains and under disease conditions deserve deeper investigation.

## REFERENCES AND NOTES

- X. Xiang, K. Wind, T. Wiedemann, T. Blume, Y. Shi, N. Briel, L. Beyer, G. Biechele, F. Eckenweber, A. Zatcepin, S. Lammich, S. Ribicic, S. Tahirovic, M. Willem, M. Deussing, C. Palleis, B.-S. Rauchmann, F.-J. Gildehaus, S. Lindner, C. Spitz, N. Franzmeier, K. Baumann, A. Rominger, P. Bartenstein, S. Ziegler, A. Drzezga, G. Respondek, K. Buerger, R. Perneczky, J. Levin, G. U. Höglinger, J. Herms, C. Haass, M. Brendel, Microglial activation states drive glucose uptake and FDG-PET alterations in neurodegenerative diseases. *Sci. Transl. Med.* **13**, eabe5640 (2021).

2. H. Choi, Y. Choi, E. J. Lee, H. Kim, Y. Lee, S. Kwon, D. W. Hwang, D. S. Lee; For the Alzheimer's Disease Neuroimaging Initiative, Hippocampal glucose uptake as a surrogate of metabolic change of microglia in Alzheimer's disease. *J. Neuroinflammation* **18**, 190 (2021).
3. S. E. Dos Santos, M. Medeiros, J. Porfírio, W. Tavares, L. Pessôa, L. Grinberg, R. E. P. Leite, R. E. L. Ferretti-Rebustini, C. K. Suemoto, W. J. Filho, S. C. Noctor, C. C. Sherwood, J. H. Kaas, P. R. Manger, S. Herculano-Houzel, Similar microglial cell densities across brain structures and mammalian species: Implications for brain tissue function. *J. Neurosci.* **40**, 4622–4643 (2020).
4. H. Fu, Y. Zhao, D. Hu, S. Wang, T. Yu, L. Zhang, Depletion of microglia exacerbates injury and impairs function recovery after spinal cord injury in mice. *Cell Death Dis.* **11**, 528 (2020).
5. R. da Andrea Silva, B. Bellaver, D. G. Souza, G. Schu, I. C. Fontana, G. T. Venturin, S. Greggio, F. U. Fontella, M. L. Schiavenin, L. S. Machado, D. Miron, J. C. da Costa, P. R. N. R. Neto, D. O. Souza, L. Pellerin, E. R. Zimmer, Clozapine induces astrocyte-dependent FDG-PET hypometabolism. *Eur. J. Nucl. Med. Mol. Imaging* 10.21203/rs.3.rs-974963/v1 (2021).
6. G. Chételat, J. Arbizu, H. Barthel, V. Garibotto, I. Law, S. Morbelli, E. van de Giessen, F. Agosta, F. Barkhof, D. J. Brooks, M. C. Carrillo, B. Dubois, A. M. Fjell, G. B. Frisoni, O. Hansson, K. Herholz, B. F. Hutton, C. R. Jack Jr., A. A. Lammertsma, S. M. Landau, S. Minoshima, F. Nobili, A. Nordberg, R. Ossenkoppele, W. J. G. Oyen, D. Perani, G. D. Rabinovici, P. Scheltens, V. L. Villemagne, H. Zetterberg, A. Drzezga, Amyloid-PET and <sup>18</sup>F-FDG-PET in the diagnostic investigation of Alzheimer's disease and other dementias. *Lancet Neurol.* **19**, 951–962 (2020).
7. S. A. Liddel, K. A. Guttenplan, L. E. Clarke, F. C. Bennett, C. J. Bohlen, L. Schirmer, M. L. Bennett, A. E. Münch, W. S. Chung, T. C. Peterson, D. K. Wilton, A. Frouin, B. A. Napier, N. Panicker, M. Kumar, M. S. Buckwalter, D. H. Rowitch, V. L. Dawson, T. M. Dawson, B. Stevens, B. A. Barres, Neurotoxic reactive astrocytes are induced by activated microglia. *Nature* **541**, 481–487 (2017).
8. B. B. Tournier, S. Tsartsalis, K. Ceyzériat, B. H. Fraser, M. C. Grégoire, E. Kövari, P. Millet, Astrocytic TSPO upregulation appears before microglial TSPO in Alzheimer's disease. *J. Alzheimers Dis.* **77**, 1043–1056 (2020).
9. N. Mirzaei, S. P. Tang, S. Ashworth, C. Coello, C. Plisson, J. Passchier, V. Selvaraj, R. J. Tyacke, D. J. Nutt, M. Sastre, In vivo imaging of microglial activation by positron emission tomography with [(11)C]JPBR28 in the 5XFAD model of Alzheimer's disease. *Glia* **64**, 993–1006 (2016).
10. B. Liu, K. X. Le, M. A. Park, S. Wang, A. P. Belanger, S. Dubey, J. L. Frost, P. Holton, V. Reiser, P. A. Jones, W. Trigg, M. F. di Carli, C. A. Lemere, In vivo detection of age- and disease-related increases in neuroinflammation by 18F-GE180 TSPO MicroPET imaging in wild-type and Alzheimer's transgenic mice. *J. Neurosci.* **35**, 15716–15730 (2015).
11. S. Herculano-Houzel, B. Mota, R. Lent, Cellular scaling rules for rodent brains. *Proceedings of the National Academy of Sciences of the United States of America* **103**, 12138–12143 (2006).
12. Y. Lei, H. Han, F. Yuan, A. Javeed, Y. Zhao, The brain interstitial system: Anatomy, modeling, in vivo measurement, and applications. *Prog. Neurobiol.* **157**, 230–246 (2017).
13. C. Lund-Andersen, Transport of glucose from blood to brain. *Physiol. Rev.* **59**, 305–352 (1979).
14. L. Sokoloff, M. Reivich, C. Kennedy, M. H. Des Rosiers, C. S. Patlak, K. D. Pettigrew, O. Sakurada, M. Shinohara, The [14C]deoxyglucose method for the measurement of local cerebral glucose utilization: theory, procedure, and normal values in the conscious and anesthetized albino rat. *J. Neurochem.* **28**, 897–916 (1977).
15. B. P. Chugh, J. P. Lerch, L. X. Yu, M. Pienkowski, R. V. Harrison, R. M. Henkelman, J. G. Sled, Measurement of cerebral blood volume in mouse brain regions using micro-computed tomography. *Neuroimage* **47**, 312–318 (2009).
16. M. F. Alf, M. T. Wyss, A. Buck, B. Weber, R. Schibli, S. D. Krämer, Quantification of brain glucose metabolism by 18F-FDG PET with real-time arterial and image-derived input function in mice. *J. Nucl. Med.* **54**, 132–138 (2013).
17. N. Meyer, N. Richter, Z. Fan, G. Siemonsmeier, T. Pivneva, P. Jordan, C. Steinhäuser, M. Semtner, C. Nolte, H. Kettenmann, Oligodendrocytes in the Mouse Corpus Callosum Maintain Axonal Function by Delivery of Glucose. *Cell Rep.* **22**, 2383–2394 (2018).

**Competing interests:** M.B. received speaker honoraria from GE Healthcare, Roche, and Life Molecular Imaging and is an advisor of Life Molecular Imaging. C.H. is the chief scientific advisor of ISAR Biosciences and collaborates with DENALI therapeutics. All other authors declare that they have no competing interests.

Submitted 1 December 2021

Accepted 12 July 2022

Published 24 August 2022

10.1126/scitranslmed.abn5104